Proceedings of the
International Meteor Conference
La Palma, Canary Islands, Spain
20–23 September, 2012

Distribution

Further copies of this publication may be ordered from the Treasurer of the International Meteor Organization, Marc Gyssens, Mattheessensstraat 60, 2540 Hove, Belgium, or through the IMO website (`http://www.imo.net`).

Bidirectional reflectance measurements of meteorites acquired by FGI's field goniospectrometer

Maria Gritsevich[1,2,3,4], Teemu Hakala[1], Jouni Peltoniemi[1], Mark Paton[5], Jarkko Stenman[6] and Arto Luttinen[6]

[1] Department of Remote Sensing and Photogrammetry, Finnish Geodetic Institute, Geodeetinrinne 2, P.O. Box 15, FIN-02431 Masala, Finland

[2] Department of Physics, University of Helsinki, Gustaf Hällströmin katu 2a, FIN-00560 Helsinki, Finland

[3] Institute of Mechanics and Faculty of Mechanics and Mathematics, Lomonosov Moscow State University, Michurinsky Pr. 1, Moscow, 119192, Russia

[4] Dorodnitsyn Computation Center of the RAS, Vavilova Ul. 40, Moscow, 119333, Russia
gritsevich@list.ru

[5] Finnish Meteorological Institute, Erik Palménin aukio 1, FIN-00560 Helsinki, Finland

[6] Finnish Museum of Natural History, University of Helsinki, Norra Järnvägsgatan 13, FIN-00100 Helsinki, Finland.

Meteorite studies represent a low-cost opportunity for probing the cosmic matter that reaches the Earth's surface, and for revealing the origin of our Solar System. In addition, they complement results of sample-return missions that bring back pristine samples of this material. The main difficulty, however, with interpreting meteorite records is that, apart from a few exceptional cases, we do not know their exact origin, i.e., the parent body a particular sample is coming from. In the present study, we provide results of multi-angular bidirectional reflectance measurements of relatively big meteorite samples, from the Finnish Museum of Natural History, using the field goniospectrometer FIGIFIGO. We discuss possible matches between our measured reflectance spectra of meteorites with the reflectance spectra of asteroids. We discuss the features in the spectra and their relationship to the physical properties of the sample/asteroid.

1 Introduction

Understanding the nature and origin of meteoroids that pass by the Earth and occasionally hit our planet helps us to predict and be prepared for possible future Near Earth Objects (NEO) impact threats. In terms of orbital elements, NEOs are asteroids and comets with perihelion distance q less than 1.3 AU[1]. Near-Earth Comets (NECs) are further restricted to include only short-period comets with orbital period P less than 200 years. The majority of NEOs are asteroids, referred to as Near-Earth Asteroids (NEAs). Thus, a number of recent studies are addressing the problem of matching meteorites to their asteroid origin based on evaluated orbits, or, when there are no good observations available to derive orbital parameters, on the basis of their mineral composition (Vernazza et al., 2008; Bland et al., 2009; Binzel et al., 2010). It is problematic to compare the meteorite and asteroid groups directly, as the meteorite collection is subject to strong selection effects. First, the strength of meteorites controls those that survive entry into the atmosphere (Ceplecha et al., 1993). Second, it is thought that there is also a selection effect due to size. Smaller meteorites are more easily transported out of the main belt due to the Yarkovsky effect (Vernazza et al., 2008) than the large NEAs. These in turn are from a few locations near resonant orbits with Jupiter. Finally, it is also thought that meteorites sample the inner main belt (Bottke et al., 2002), although it is possible that meteorites can travel from further out (Nesvorný et al., 2009). The metamorphic evolution of asteroids is preserved within the meteorite collection and can give us information on differentiated asteroids such as in the case of Vesta with the HED group of meteorites (McCord et al., 1970).

Some good matches have been made between individual meteorite spectra and NEAs (McFadden et al., 1985) as well as between meteorite spectra and large main belt asteroids (Binzel and Xu, 1993). The principle properties of the spectra used to identify possible matches between meteorites and asteroids are the band minimum location and Band Area Ratio (BAR). The band minimum is the wavelength location of an absorption band in the spectra. The BAR is the ratio between the area of the bands in the spectra. These properties are diagnostic of the object's mineralogy and, to lesser extend, of other physical properties such as surface roughness and grain size (e.g., Paton et al., 2011). The spectra of meteorites and asteroids are also dependent on observational conditions such as the phase angle between the line connecting the light source (e.g., the Sun) with the target and the line connecting the target with the observer. This is a key effect that needs to be under-

---

[1] http://neo.jpl.nasa.gov/neo.html.

stood to help improve matches between meteorites and asteroids, as this phase angle, when observing asteroids, varies due to the ever changing orbital positions of viewer and target. Variations in the band depths, band minimum locations, the band area ratio, and spectral slope have been noted to vary with phase angle and have been characterized (Sanchez et al., 2012). Although this effect does not seem to affect the mineralogical analysis very much, it is important for understanding optical effects and their relationship to physical properties such as surface roughness and grain size.

2   What is BRF?

The surface reflectance is described by its bidirectional reflectance factor (BRF). BRF is defined as a ratio of the reflected light intensity of a given target to an ideal Lambertian reflector with a spherical albedo of 1.0 under the same incident irradiance:

$$R(\mu, \mu_0, \phi, \phi_0) = \frac{\pi I(\mu, \phi)}{\mu_0 F_0(\mu_0, \phi_0)}, \qquad (1)$$

with F_0 the incident collimated flux $(I_0(\Omega) = F_0 \delta(\Omega - \Omega_0))$ and I the reflected radiance. The definitions of the angles are visualized in Figure 1: ι and ϕ_0 are the zenith and azimuth angles of incidence, ε and ϕ are the zenith and azimuth angles of emergence, α is the scattering phase angle $(\cos\alpha = \cos\iota\cos\varepsilon + \sin\iota\sin\varepsilon\cos(\phi - \phi_0))$, a complement of the scattering angle. One can further define the specular direction, $(\iota, -\phi_0)$, and the angle from that direction, γ.
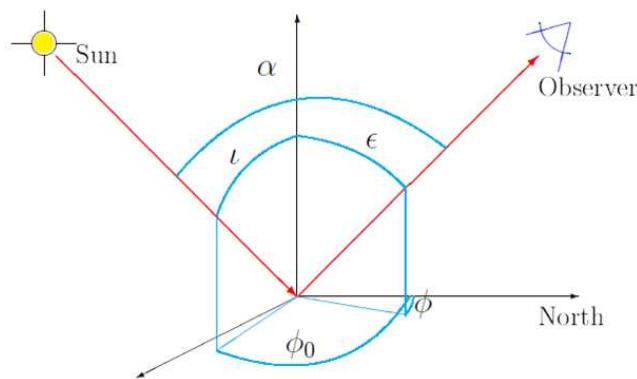
Figure 1 – Definition of the angles used in surface reflectance work: ε and ι are the zenith angles of the emergent (observer) and incident (solar) radiation, respectively (shorthands $\mu = \cos\varepsilon$ and $\mu_0 = \cos\iota$ are also used). The angles ϕ and ϕ_0 are the corresponding azimuths. The phase or back scattering angle α is the angle between the observer and the Sun. The principal plane is fixed by the solar direction and the surface normal, while the cross plane is a vertical plane perpendicular to the principal plane.

From its definition (1), it follows that BRF is a function of four angles, but, if the target is sufficiently horizontally/azimuthally isotropic, the functional dependence is reduced to three variables, as the only azimuthal variable is the difference $(|\phi - \phi_0|)$.

Albedo, or reflection coefficient, is defined as a ratio of all reflected (scattered) radiance to all incident irradi-

ance. Being a dimensionless fraction, albedo may also be expressed as a percentage, and it is measured on a scale from zero for no reflecting power of a perfectly black body, to 1 for perfect reflection of a white surface. Depending on the application, there are many variations of the definition of the albedo, and thus one needs to be careful applying formulae from another field. The albedo is related to BRF as

$$A = \frac{\int d\lambda \int d\phi d\mu \int d\phi_0 d\mu_0 \, R(\mu, \phi, \mu_0, \phi_0, \lambda) I_0(\mu_0, \phi_0, \lambda)}{\int d\lambda \int d\phi_0 d\mu_0 \, I_0(\mu_0, \phi_0, \lambda)}.$$
$$(2)$$

Albedo is thus a function of the incident light distribution. Often, one defines directionally and spectrally resolved albedo

$$A_r(\mu_0, \phi_0, \lambda) = \frac{\int d\phi d\mu \, R(\mu, \phi, \mu_0, \phi_0, \lambda)}{\pi} \qquad (3)$$

that is a property of the surface. In principle, the integrations in (2) run over full hemispheres and wavelength ranges, but, in many practical applications, the observational range may be limited to smaller wavelength ranges, e.g., only optical or visual bands, and the field of view of the instrument is also often limited (typical albedometers see zenith angle ranges of $70°$ to $80°$).

BRFs of typical remote sensing targets vary by a large scale. Some targets are forward scatterers, some are backscatterers, some have a strong specular reflection, and some reflect highly to low zenith angles (Peltoniemi, 2007; Peltoniemi et al., 2009; 2005a; 2005b). Each target has its unique BRF that depends on all of its geometrical and physical properties. Thus, exploitation of BRF information is a valuable tool in target classification and quantification.

3   Instrumentation

The meteorite BRF measurements have been taken using the Finnish Geodetic Institute field foniospectrometer Figifigo, an automated portable instrument for multi-angular reflectance measurements (see Figures 2 and 3). The Figifigo system consists of a motor-driven moving arm that tilts up to about $90°$ from the vertical, for optics in the high end of the arm, and an ASD Field-Spec Pro FR 350–2500 nm spectroradiometer. Accurate zenith angles are read with an inclinometer, and an all-sky camera is used to orient the system azimuth angle to the Sun. The detailed description of the instrument is provided by Hakala (2009).

Typically, the footprint diameter is about 10 cm, elongating at larger sensor zenith angles as $1/\cos\theta$, and wandering around a few centimeters by bending and with azimuthal movements. A motorized fine-tune mirror is installed to correct paraxial and bending errors and to keep the measurement point stable to an accuracy of 2 cm.

All the measurements were taken from $0°$ relative azimuth (principal plane). Due to the small target size, the zenith angles were restricted to approximately $60°$.
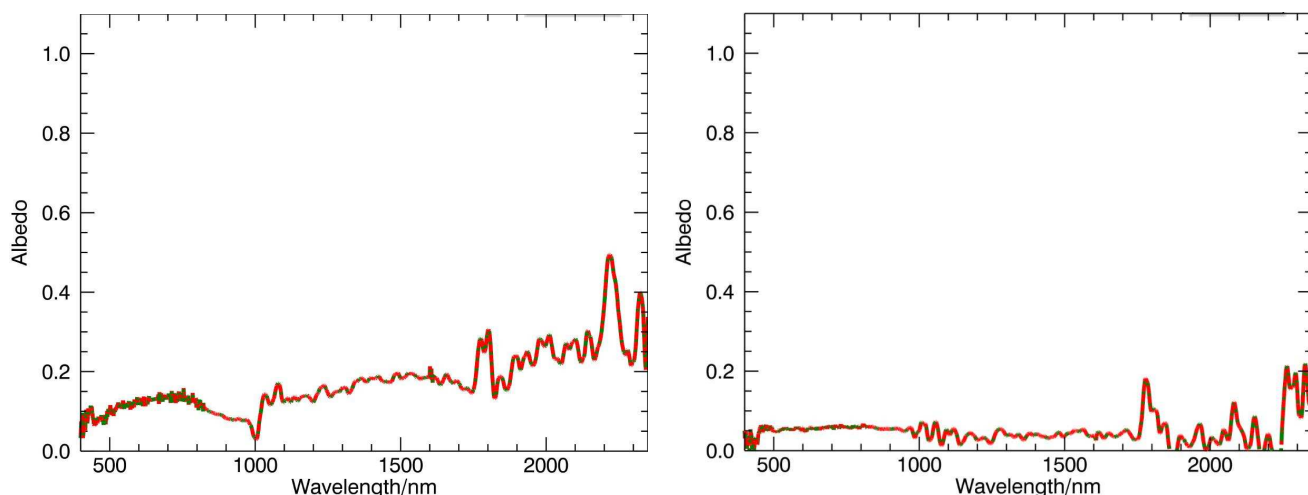
Figure 2 – Examples of measured albedo: Bruderheim meteorite, cut (a) and rough surface (b).

Figure 3 – FIGIFIGO measuring the BRF of a selected sample. FIGIFIGO consists of casing, measurement arm, and rugged computer. The casing contains the main sensor ASD FieldSpec Pro FR optical fibre spectroradiometer (350–2500 nm), most of the electronics, and batteries. The telescopic measurement arm is adjustable from 1.55 to 2.65 m, and houses an inclinometer to provide the control computer with the measurement of the zenith angle. At the top of the measurement arm, there is the active optics system. The optics views the sample through a servo-driven mirror. The turnable mirror allows the control computer to stabilize the spectrometer field-of-view at the sample within accuracy of 2 cm from all zenith directions, even if the sample is not positioned exactly at the center of rotation.

The measurement arm was first driven to maximum angle, and then slowly to minimum angle, while continuously collecting spectra. The instrument was calibrated by taking a nadir measurement from a Labsphere Spectralon white reference panel before and after each sequence. The Spectralon has been carefully leveled at horizontal with a bubble level with an accuracy of 1°. The accuracy of the spectral BRF measurements using FIGIFIGO is estimated to be 2–3% in the visible band and good conditions. Angle registration accuracy is 2°. In data processing the measured unnormalized radiance spectra S are normalized by the measured nadir spectrum from a reference target (S_{STD}) as

$$R(\mu, \mu 0, \phi, \phi_0) = \frac{S}{S_{\mathrm{STD}}} R_{\mathrm{STD}}, \qquad (4)$$

where R_{STD} is the reflectance of the reference target.

4 Selected meteorite samples

The summary of the meteorite samples selected for measurements from the Finnish Museum of Natural History (Geological Museum) is presented in Table 1. The meteorite exhibition belongs to the Geological Museum and is on display at the Mineral Cabinet in association with the Helsinki University Museum[2].

5 Features in the spectra and sample relationship to asteroids

The results of our measurements are partly summarized in Figure 4 for the Bruderheim L6 chondrite. The spectra are obtained at different zenith angles. These show a general reddening of the spectra as the absolute zenith angle increases.
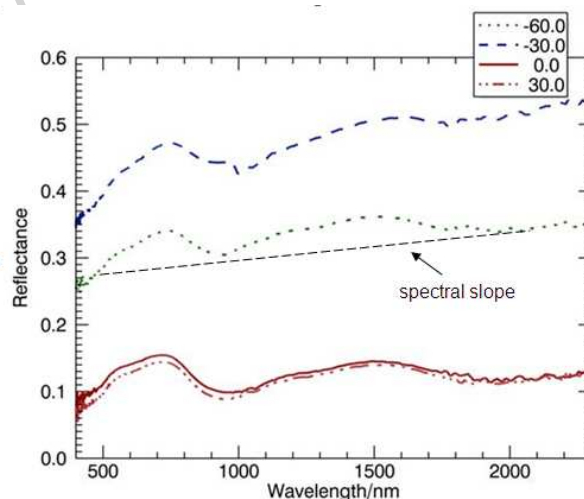
Figure 4 – Spectra from the Bruderheim meteorite for a variety of zenith angles in the principal plane.

One could plot the slope gradients, as defined in Figure 4, for a variety of meteorites which may have either a rough surface, a non-rough surface, or a smooth

Table 1 – Summary of meteorite samples selected for measurements from the Finnish Museum of Natural History (Geological Museum).

Name	Observed fall?	Year found	Country	Classification	Total mass found
Bruderheim	March 4, 1960	1960	Canada	L6	303 kg
Canyon Diablo	No	1891	United States	Iron, IAB-MG	30×10^3 kg
Cape York	No	1818	Greenland	Iron, IIIAB	58.2×10^3 kg
Charcas	No	1804	Mexico	Iron, IIIAB	1.4×10^3 kg
Gibeon	No	1836	Namibia	Iron, IVA	26×10^3 kg
Marjalahti	June 1, 1902	1902	Russia	Pallasite, PMG	45 kg

surface. Here, a "rough surface" refers to large-scale roughness of the original surface of the meteorite, which may contain pits due to ablation effects, or has a generally rocky appearance. A "non-rough surface" is then a flat sawn surface. This may contain small pits and cracks in its surface. A "smooth surface" is a flat polished surface. Based on our measurements, the slope gradients for a given zenith angle are clearly higher for non-rough surfaces than for rough surfaces. This is consistent with previous work that observed overall reduction in reflected light and the flattening of the spectrum (more blue) due to decreasing reflectance with increasing wavelength, for rough dielectric surfaces (e.g., Yon and Pieters, 1988).

For the non-rough surface of the Bruderheim L6 chondrite, the gradient of the spectral slope increases with decreasing (i.e., more negative) zenith angle. The absolute value of the zenith angle in the principal plane may be thought of as analogous to a phase angle. This then follows a similar trend found previously (Sanchez et al., 2007) where the spectral slope gradient, for various chondrites (including L6) was found to increase significantly with increasing phase angle. The spectral slope gradient is known to increase for S-type asteroids (e.g., Natheus, 2010) which are linked to ordinary chondrite meteorites. Similar trends of increasing slope gradient, increasing with decreasing zenith angles, are observed for the measured iron meteorites in Table 1, except for the Marjalahti, Cape York, and Gibeon meteorites, which have flat spectra and appear to remain more or less flat with decreasing zenith angle.

6   Conclusions

Exploitation of BRF information is proved to be a valuable tool when applied to meteorite studies and their relationship to the physical properties of asteroids. In particular, we have observed the spurious variations in the spectra for the Bruderheim meteorite, especially around 0.9 and 1.8 μm. Absorption bands have to be expected in these regions for L6 meteorite types. L chondrites are a sub category of ordinary chondrites, which are linked to S-type asteroids. For L chondrites, the spectral slope, as defined here, increases its gradient with increasing absolute zenith angle, and follows a similar trend as the spectral slopes of S-type asteroids, whose gradient increases with increasing phase angle.

The spectral slopes of the iron meteorites generally have an opposite trend than those of our chondrite measurements.

References

Binzel R. P., Morbidelli A., Merouane S., Demeo F. E., Birlan M., Vernazza P., Thomas C. A., Rivkin A. S., Bus S. J., and Tokunaga A. T. (2010). "Earth encounters as the origin of fresh surfaces on near-Earth asteroids". *Nature*, **463**, 331–334.

Binzel R. P. and Xu S. (1993). "Chips off of asteroid 4 Vesta: evidence for the parent body of basaltic achondrite meteorites". *Science*, **260**, 186–191.

Bland P. A., Spurný P., Towner M. C., Bevan A. W. R., Singleton A. T., Bottke W. F. Jr., Greenwood R. C., Chesley S. R., Shrbený L., Borovička J., Ceplecha Z., McClafferty T. P., Vaughan D., Benedix G. K., Deacon G., Howard K. T., Franchi L. A., and Hough R. M. (2009). "An anomalous basaltic meteorite from the innermost main belt". *Science*, **325**, 1525–1527.

Bottke W. F. Jr., Vokrouhlický D., Rubincam D. P., and Brož M. (2002). "The effect of Yarkovsky thermal forces on the dynamical evolution of asteroids and meteoroids". In Bottke W. F. Jr., Cellino A., Paolicchi P., Binzel R. P., editors, *Asteroids III*, Univ. of Arizona Press, pages 395–408.

Ceplecha Z., Spurný P., Borovička J., and Keclikova J. (1993). "Atmospheric fragmentation of meteoroids". *Astron. & Astrophys.*, **279**, 615–626.

Hakala T. (2009). *Improvements, Calibration, and Accuracy of the Finnish Geodetic Institute Field Goniospectrometer.* M. Sc. Thesis, Helsinki University of Technology.

McCord T. B., Adams J. B., and Johnson T. V. (1970). "Asteroid Vesta: spectral reflectivity and compositional implications". *Science*, **168**, 1445–1447.

McFadden L. A., Gaffey M. J., and McCord T. B. (1985). "Near-Earth asteroids: possible sources from reflectance spectroscopy". *Science*, **229**, 160–163.

Nathues A. (2010). "Spectral study of the Eunomia asteroid family. Part II: The small bodies". *Icarus*, **208**, 252–275.

Nesvorný D., Vokrouhlický D., Morbidelli A. and Bottke W. F. (2009). "Asteroidal source of L chondrite meteorites". *Icarus*, **200**, 698–701.

Paton M. D., Muinonen K., Pesonen L. J., Kuosmanen V., Kohout T., Latinen J., and Lehtinen, M. (2011). "A PCA study to determine how features in meteorite reflectance spectra vary with the samples' physical properties". *Journal of Quantative Spectroscopy and Radiative Transfer*, **112**, 1804–1814.

Peltoniemi J. I. (2007). "Spectropolarised ray-tracing simulations in densely packed particulate medium". *Journal of Quantative Spectroscopy and Radiative Transfer*, **108**, 180–196.

Peltoniemi J., Hakala T., Suomalainen J., and Puttonen E. (2009). "Polarised bidirectional reflectance factor measurements from soil, stones, and snow".

Journal of Quantative Spectroscopy and Radiative Transfer, **110**, 1940–1953.

Peltoniemi J. I., Kaasalainen S., Näränen J., Matikainen L., and Piironen J. (2005a). "Measurement of directional and spectral signatures of light reflectance by snow". *IEEE Transactions on Geoscience and Remote Sensing*, **43**, 2294–2304.

Peltoniemi J. I., Kaasalainen S., Näränen J., Rautiainen M., Stenberg P., Smolander H., Smolander S., and Voipio P. (2005b). "BRDF measurement of understory vegetation in pine forests: dwarf shrubs, lichen, and moss". *Remote Sensing of Environment*, **94**, 343–354.

Sanchez J. A., Reddy V., Nathues A., Cloutis E. A., Mann P., and Hiesinger H. (2012). "Phase reddening on near-Earth asteroids: implications for mineralogical analysis, space weathering and taxonomic classification". *Icarus*, **220**, 36–50.

Vernazza P., Binzel R. P., Thomas C. A., DeMeo F. E., Bus S. J., Rivkin A. S., and Tokunaga A. T. (2008). "Compositional differences between meteorites and near-Earth asteroids". *Nature*, **454**, 858–860.

Yon S. A. and Pieters C. M. (1988). "Interactions of light with rough dielectric surfaces—spectral reflectance and polarimetric properties". In *Proceedings 18th Lunar and Planetary Science Conference*, Houston, Texas, March 16–20, 1987 (A89-10851 01-91), Cambridge University Press/Lunar and Planetary Institute, pages 581–592.